Endogenous dynorphin in epileptogenesis and epilepsy: anticonvulsant net effect via kappa opioid receptors

Stephan Loacker,[1] Mohammad Sayyah,[1,*] Walter Wittmann,[1] Herbert Herzog[2] and Christoph Schwarzer[1]

[1]Department of Pharmacology, Innsbruck Medical University, Innsbruck, Austria,
[2]Neurobiology Program, Garvan Institute of Medical Research, St Vincent's Hospital, Sydney, Australia
*Present address: Department of Physiology and Pharmacology, Pasteur Institute of Iran, Pasteur avenue, Tehran, Iran

Correspondence to: Dr Christoph Schwarzer, Department of Pharmacology, Innsbruck Medical University, Peter-Mayr-Str. 1a, A-6020 Innsbruck, Austria
E-mail: schwarzer.christoph@i-med.ac.at

Neuropsychiatric disorders are one of the main challenges of human medicine with epilepsy being one of the most common serious disorders of the brain. Increasing evidence suggest neuropeptides, particularly the opioids, play an important role in epilepsy. However, little is known about the mechanisms of the endogenous opioid system in epileptogenesis and epilepsy. Therefore, we investigated the role of endogenous prodynorphin-derived peptides in epileptogenesis, acute seizure behaviour and epilepsy in prodynorphin-deficient mice. Compared with wild-type littermates, prodynorphin knockout mice displayed a significantly reduced seizure threshold as assessed by tail-vein infusion of the GABA$_A$ antagonist pentylenetetrazole. This phenotype could be entirely rescued by the kappa receptor-specific agonist U-50488, but not by the mu receptor-specific agonist DAMGO. The delta-specific agonist SNC80 decreased seizure threshold in both genotypes, wild-type and knockout. Pre-treatment with the kappa selective antagonist GNTI completely blocked the rescue effect of U-50488. Consistent with the reduced seizure threshold, prodynorphin knockout mice showed faster seizure onset and a prolonged time of seizure activity after intracisternal injection of kainic acid. Three weeks after local injection of kainic acid into the stratum radiatum CA1 of the dorsal hippocampus, prodynorphin knockout mice displayed an increased extent of granule cell layer dispersion and neuronal loss along the rostrocaudal axis of the ipsi- and partially also of the contralateral hippocampus. In the classical pentylenetetrazole kindling model, dynorphin-deficient mice showed significantly faster kindling progression with six out of eight animals displaying clonic seizures, while none of the nine wild-types exceeded rating 3 (forelimb clonus). Taken together, our data strongly support a critical role for dynorphin in the regulation of hippocampal excitability, indicating an anticonvulsant role of kappa opioid receptors, thereby providing a potential target for antiepileptic drugs.

Introduction

With a prevalence of 1–2% epilepsies are one of the most frequent neurological diseases (McNamara, 1999). According to the WHO, 50 million people are affected world-wide, thereby accounting for 1% of global burden of disease (WHO, 2005). About 70% of all epilepsy patients suffer from focal seizures, arising from a distinct brain region. Mesial temporal lobe epilepsy (mTLE) is, to our present knowledge, the most frequent type of epilepsy.

Although 10 new antiepileptic drugs were made available since the late 1980s, refractoriness to treatment is still an important issue in epilepsy care. Only two-thirds of patients are seizure-free under pharmacological treatment (Kwan and Brodie, 2000; Kwan and Sander, 2004). Presently, surgical resection of the epileptogenic focus remains as an alternative therapy (Nilsen and Cock, 2004; Polkey, 2004). Although highly effective, this represents an invasive

treatment. Thus, new therapeutical strategies are needed, and might be found in the field of neuropeptides.

The number of studies supporting the importance of neuropeptides in epileptogenesis and epilepsy are increasing. Since the early 1980s, there is evidence that opioids, namely dynorphin, act as modulators of neuronal excitability in vitro (Henriksen et al., 1982; Siggins et al., 1986; Wagner et al., 1993; Weisskopf et al., 1993). Like the other classical opioid peptides, dynorphin exerts its actions through three opioid receptors named kappa (KOR), mu (MOR) and delta (DOR), with highest affinity to KOR (Chavkin et al., 1982). However, since the 1990s, also non-opioid effects of dynorphin (defined through insensitivity to naloxone) were reported, mainly depending on direct actions on NMDA receptors (for review see Wollemann and Benyhe, 2004). Potentiation of endogenous anti-ictal mechanisms by opioids was shown in animal models of epilepsy (Tortella, 1988; Tortella and Long, 1988; Terman et al., 2000), including viral-induced seizures (Solbrig et al., 2006), and low dynorphin expression in man is associated with increased epilepsy vulnerability (Stogmann et al., 2002; Gambardella et al., 2003). Mostly, these effects were attributed to KOR function. On the other hand, KORs are rare in the hippocampus (Maggi et al., 1989; DePaoli et al., 1994; Gackenheimer et al., 2005), which represents the central element of mTLE. In addition, application of KOR-specific agonists and antagonists does neither address the involvement of potential proconvulsant effects mediated through MOR located on GABAergic interneurons nor the induction of seizures by DOR agonists nor non-opioid effects on NMDA receptor functions.

In fact, till now very little information is available on the role of endogenous dynorphin in epileptogenesis and seizure behaviour. It is still controversial, whether the net effect of prodynorphin-derived peptides acting on DOR, KOR, MOR and/or NMDA receptors is pro- or anti-convulsant. On the other hand, we need detailed knowledge of the physiological and pathophysiological role of the opioid system to develop strategies for novel treatments. To address these issues, we investigated prodynorphin-deficient mice in animal models of epileptogenesis and acute seizures.

Material and methods
Targeting vector construction and gene disruption
The coding sequence for the transactivator of the Tet-on system (rTetR) was introduced directly after the ATG of the prodynorphin gene using an XbaI site, which was mutated into the prodynorphin sequence by means of polymerase chain reaction (PCR) (mutating reverse primer: 5′-GCTCTAGACATTCTGACTCACTTGTTTG-3′). The sequence for the transactivator responsive element (TRE) was placed against the prodynorphin reading direction, driving Cre-recombinase expression. In the same direction, we placed a loxP site flanked cassette containing neomycin and zeocin resistance genes. The targeting construct for transfection of embroyonic stem (cells) was flanked by about 4 kB

genomic fragments directly upstream to the ATG on exon 3 and about 2.5 kB downstream of exon 4. Genomic DNA fragments were obtained from a Lambda clone kindly provided by Dr Ute Hochgeschwender. BstEII and HindIII were used for 5′ and 3′ Southern blot screening for correct insertions of the targeting construct in 129/SvJ embryonic stem cells. Two positive clones were injected into C57Bl/6 blastocysts. Chimeric mice were bred with C57Bl/6 mice to generate heterozygous knockout mice (Dyn$^{+/-}$). Breeding the heterozygous mice generated all three possible genotypes (Dyn$^{-/-}$; Dyn$^{+/-}$; Dyn$^{+/+}$). The genotype of mice was determined by Southern blot analysis as described in the Results section, and by PCR using oligonucleotides A (5′-GGCTTCTCATCTTTTCTCACCC-3′) and B (5′- TCACCACCTTGAACTGACGC-3′) situated on exon 4 of the prodynorphin gene and oligonucleotides C (5′-CCACGACCAAGTGACAGCAATG-3′) and D (5′-AAGTGCCTTCTCTACACCTGCG-3′) situated on the Cre-recombinase sequence, with 35 cycles of 94°C for 45 s, 58°C (Dyn) or 56°C (Cre) for 45 s and 72°C for 45 s.

Animals
Mice were backcrossed onto the C57Bl/6N background over eight generations and littermates were used as controls. No obvious differences in fertility, body weight or behaviour were observed between wild-type and knockout animals. Male mice at 12–16 weeks were tested in all experiments. All procedures involving animals were approved by the Austrian Animal Experimentation Ethics Board in compliance with the European Convention for the Protection of Vertebrate Animals used for Experimental and Other Scientific Purposes (ETS no. 123). Every effort was taken to minimize the number of animals used.

Real-time polymerase chain reaction (RT-PCR)
RT-PCR was performed on cDNA gained from entire hippocampal mRNA extracts. The mRNA was isolated using oligo-dT primers covalently coupled to magnetic beads (DynalBiotech, Hamburg, Germany) and transcribed to cDNA using Superscript II reverse transcriptase^{TM} and oligo(dT)12–18 primers (both Invitrogen, Lofer, Austria) using standard protocols. Taqman primer sets for the amplification of DOR, KOR and MOR (Applied Biosystems # Mn00443063_m1; Mn00440561_m1; Mn01188089_m1, respectively) and the mouse TATA box binding protein (mTBP489f: 5′-ACTTCGTGCAAGAAATGCTGAA-3′; mTBP564r: 5′-TGTCCGTGGCTCTCTTATTCTCA-3′; mTBP Probe: 5′-TCCCAAGCGATTTGCTGCAGTCATC-3′) cDNAs as internal standard were used. Amplification was carried out on ABI Prism 7500 Fast Real-Time PCR System (Applied Biosystems, Foster City, CA) using Taqman Universal PCR Mastermix (Applied Biosystems) according to the manufacturer's instructions. Primers and probes were used at a final concentration of 800 nM and 150 nM respectively. Reactions were carried out in optical 96-well fast reaction plates (Applied Biosystems) in triplicate with 11 µl reaction volume containing a total of 3 ng of reverse-transcribed mRNA. Data are given as mean dCt of the three replicates calculated from receptor cDNA and respective mTBP cDNA amplification curves.

Seizure threshold
Seizure threshold was determined by pentylenetetrazole (PTZ) tail-vein infusion on freely moving animals at a rate of 100 µl/min

(100 µg/ml PTZ in saline, pH 7.4). Infusion was stopped when animals displayed generalized clonic seizures. Animals were immediately anaesthetized using increasing carbon dioxide concentrations and killed by cervical displacement. The seizure threshold dose was calculated from the infused volume in relation to body weight. Results from tail-vein infusion were verified by intraperitoneal injection of a fixed dose of 30 mg PTZ/kg body weight. Animals were observed and video-tracked for 20 min after treatment and the severity of seizures was rated: no response = 0; immobility = 1; myoclonic jerks = 2; forelimb clonus and/or Straub tail = 3; generalized clonic seizure = 4; clonic seizures with jumping and running = 5; death = 6.

Opioid receptor pharmacology

The KOR agonist *trans*-(±)-3,4-dichloro-*N*-methyl-*N*-[2-(1-pyrrolidinyl)cyclohexyl] benzeneacetamide hydrochloride (U-50488), the KOR antagonist 5′-guanidinyl-17-(cyclopropylmethyl)-6,7-dehydro-4,5α-epoxy-3,14-dihydroxy-6,7-2′,3′-indolomorphinan dihydrochloride (GNTI), the DOR agonist (+)-4-[(aR)-a-((2S,5R)-4-allyl-2,5-dimethyl-1-piperazinyl)-3-methoxybenzyl]-*N*,*N*-diethylbenzamide (SNC80) and the MOR agonist [D-Ala^2, NMePhe^4, Gly-ol]-enkephalin (DAMGO) were purchased from Tocris Cookson. KOR and MOR ligands were dissolved in saline and pH was adjusted to 7.2. SNC80 was dissolved in 1 Eq HCl. U-50488 (20 mg/kg) and SNC80 (2 mg/kg) were applied i.p. 30 and 60 min before testing, respectively. GNTI (3 nmol) and DAMGO (2 nmol) were given intracisternally under mild sevofluorane anaesthesia 20 h and 30 min before testing, respectively. Drug doses and application times were chosen according to recent studies in mice (Yokoyama *et al.*, 1992; Jewett *et al.*, 2001; Khavandgar *et al.*, 2002; Manocha *et al.*, 2003; Solbrig *et al.*, 2006). GNTI was preferred over nor-binaltorphimine (nor-BNI) for its higher KOR selectivity and antagonist potency (Jones and Portoghese, 2000).

Seizure onset and duration

Delay until seizure onset and duration of clonic seizure activity was analysed in the kainic acid (KA) model. KA (0.7 µg in 3.5 µl saline, pH = 7.2) was injected intracisternally under very mild sevofluorane anaesthesia. Animals were observed for a minimum of 60 or 10 min after the last clonic seizures. Subsequently, animals were immediately anaesthetized using increasing carbon dioxide concentrations and killed by cervical displacement. Delay time until the first clonus and the timespan from the beginning of the first to the end of the last clonic seizures was measured from video recordings.

Intrahippocampal injections of KA

To study neuronal degeneration and hippocampal reorganization, KA was injected into the dorsal hippocampus of deeply anaesthetized (initial: Ketasol 2 mg/kg, maintenance: inhalation of sevofluorane) mice (Bouilleret *et al.*, 1999). Mice were immobilized in a stereotaxic instrument (David Kopf Instruments, Tujunga, CA) with the nose bar adjusted to equal heights of lambda and bregma. Coordinates from bregma (1.8 mm anterior; 1.6 mm lateral and 1.8 mm below skull) were chosen to target the stratum radiatum of CA1 in the right dorsal hippocampus (Paxinos and Franklin, 2001). KA (0.2 µg in 50 nl saline, pH 7.2) was applied with a 1 µl Hamilton syringe over a period of 2 min. The needle was kept in place for 5 min and

retracted stepwise (0.3 mm/min) to minimize backflux. Animals were killed 3 weeks after KA injection by an overdose of thiopental (150 mg/kg) and brains were fixed by transcardial perfusion with 4% paraformaldehyde.

PTZ kindling

Two groups of mice (Dyn$^{-/-}$ and Dyn$^{+/+}$) received up to 16 i.p. injections of 20 mg/kg PTZ over 5 weeks (Monday, Wednesday, Friday). The PTZ dose was established in a pre-experiment on wild-type mice. Animals were observed and video-tracked for 20 min after each treatment, and the severity of seizures was rated as described for the fixed PTZ dose injection. Animals exposing three subsequent rating 4 seizures were stated fully kindled, and received no further injections. After the last kindling session, animals were anaesthetized using increasing carbon dioxide concentrations and killed by cervical displacement.

Histology and cell counts

In situ hybridization was performed on 20 µm sections of fresh frozen tissue applying a ^{35}S-α-dATP-labelled DNA oligonucleotide (5′-GTTCTCCTGGGACCGCGTCACC ACCTTGAACTGACGCCG CAG -3′) complementary to prodynorphin mRNA as published recently (Lin *et al.*, 2006). For immunocytochemistry and Nissl staining, the entire hippocampal region of paraformaldehyde-fixed tissue (Paxinos and Franklin, 2001) was cut to 40 µm free-floating sections. Series containing every 6th section were stained applying specific antibodies for prosomatostatin, chromogranin B, neuropeptide Y or dynorphin A using a horseradish peroxidase conjugated secondary antibody and 3,3′-diaminobenzidine for detection (Schwarzer *et al.*, 1996, 2001). One series of sections were used for Nissl staining (Paxinos and Franklin, 2001). Cell counts and measurement of granule cell layer (GCL) area were done from sections of the dorsal hippocampus, assigned to levels from 1.3 to 2.7 mm from bregma according to Paxinos and Franklin (2001). Sections from 4 to 6 brains were evaluated for each level and the mean value taken for stereological and statistical analysis. For untreated animals, values for both hippocampi were averaged. Somatostatin immunoreactive (SST-ir) neurons were counted in the entire hippocampal subfields of the hilus, CA1 and CA3, respectively. Cell numbers of principal cell layers (CA1, CA3a, CA3b, CA3c) were assessed over a length of 125 µm covering the whole width of the layer. Specific areas counted are indicated in Fig. 3B. Granule cell dispersion was evaluated from photomicrographs through measurement of the area of the entire GCL.

Statistical analysis

For seizure threshold, pathological and pharmacological analyses, ANOVA with *post hoc* Bonferroni test was applied. For stereological analyses paired Student's *t*-test was used for comparison of genotypes at each level of the rostro-caudal axis. For RT-PCR, seizure onset and duration, unpaired Student's *t*-test was used for the comparison of wild-type and knockout animals. In the kindling experiment, and after injection of fixed PTZ doses, the χ^2 test was used to compare frequencies of seizure ratings observed in wild-type and knockout mice.

Results

Generation of germ-line prodynorphin knockout mice

A targeting vector for the prodynorphin gene was designed and generated, which allowed the replacement of the coding sequence of the prodynorphin gene by a construct expressing Cre-recombinase under the control of the Tet-on system (Supplementary Fig. 1A).

Absence of prodynorphin coding sequence in homozygote $Dyn^{-/-}$ mice was confirmed by Southern blot analysis employing a prodynorphin gene sequence-specific DNA fragments and PCR (Supplementary Fig. 1B and C, respectively).

To confirm that our construct provided entire loss of prodynorphin mRNA and protein, we performed *in situ* hybridization and immunocytochemistry experiments on brain slices from wild-type and knockout animals. As shown in Fig. 1A, wild-type mice showed significant expression of prodynorphin mRNA in the striatum, hypothalamus and hippocampus, whereas no signal was obtained in knockout animals. Wild-type mice showed significant dynorphin A immunoreactivity in nuclei also expressing prodynorphin mRNA, while knockout animals displayed no specific labelling (Supplementary Fig. 1D). Although the endogenous ligand with the highest affinity for KOR was lacking in $Dyn^{-/-}$ mice (Supplementary Fig. 1E), no obvious difference in KOR immunoreactivity was evident comparing the staining pattern in sections from the dorsal or ventral hippocampus (Fig. 1B).

Data obtained from RT-PCR show that DOR cDNA was expressed about 10 and 15 times more than KOR and MOR cDNAs, respectively (Fig. 1A). Changes in cDNA levels were minor for DOR and KOR. MOR cDNA was increased by ~40% ($P = 0.0206$; Fig. 1A) in $Dyn^{-/-}$ mice.
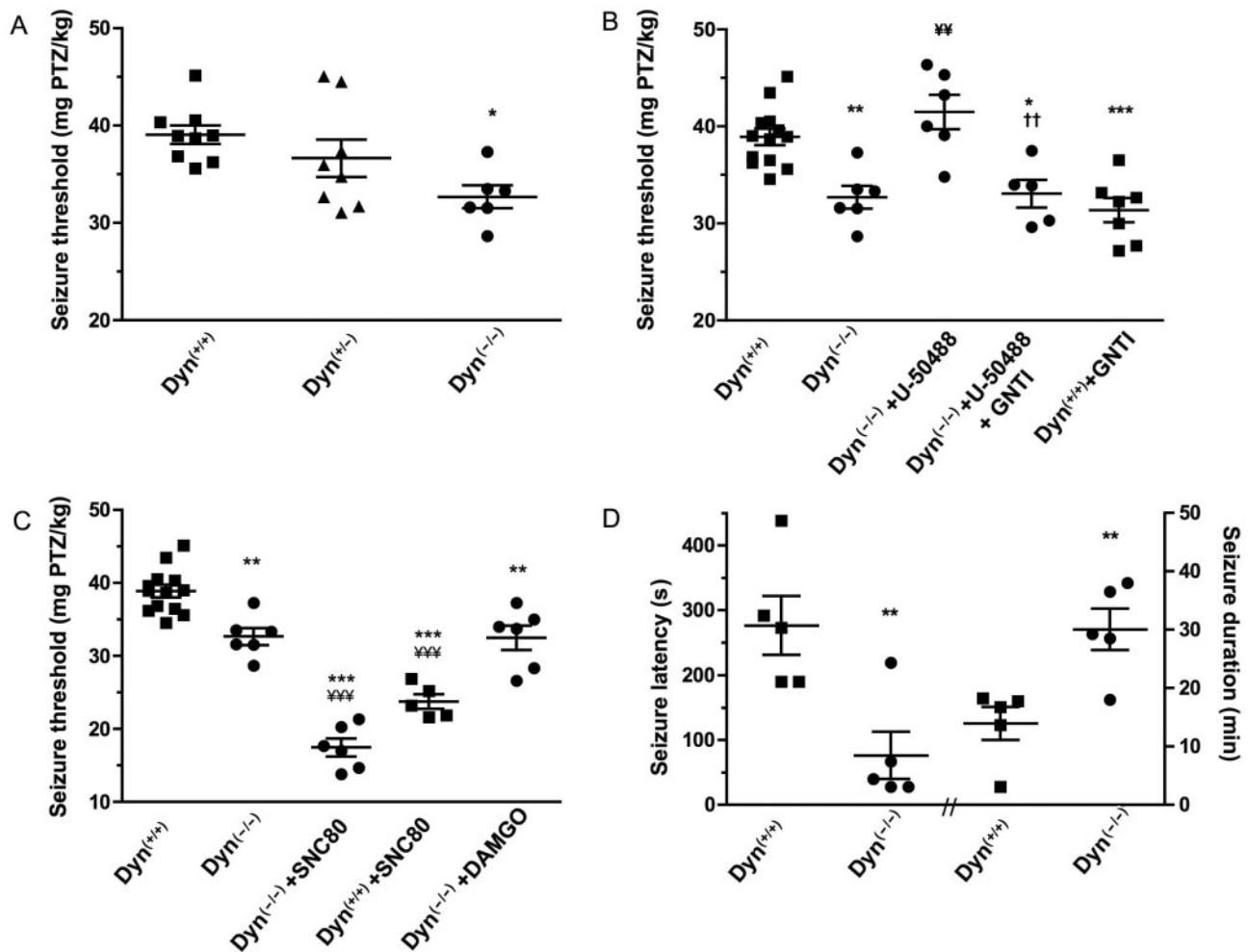
Seizure threshold

Seizure threshold was assessed by tail-vein infusion of PTZ (1 mg/min). Wild-type mice showed clonic seizures at 39.1 ± 0.96 mg PTZ/kg ($n = 9$) body weight. Prodynorphin knockouts displayed a significantly ($P < 0.05$) reduced seizure threshold of 32.7 ± 1.17 mg PTZ/kg ($n = 6$) (Fig. 2A). Heterozygous mice displayed an intermediate seizure threshold (36.7 ± 1.93; $n = 8$). A similar seizure threshold as in $Dyn^{-/-}$ was measured in wild-type mice pre-treated with the KOR-specific antagonist GNTI (3 nmol i.c.) 20 h before PTZ infusion (31.4 ± 1.25; $n = 6$). The reduced seizure threshold of $Dyn^{-/-}$ mice could be fully rescued by pretreatment with the KOR agonist U-50488 (20 mg/kg; 30 min before PTZ), yielding a threshold of 41.5 ± 1.77 ($n = 6$). This rescue effect was completely reversed by treating the mice with GNTI (3 nmol i.c.) 20 h before agonist application (33.1 ± 1.43 mg PTZ/kg; $n = 6$; Fig. 1B). Treatment of $Dyn^{-/-}$ mice with the DOR
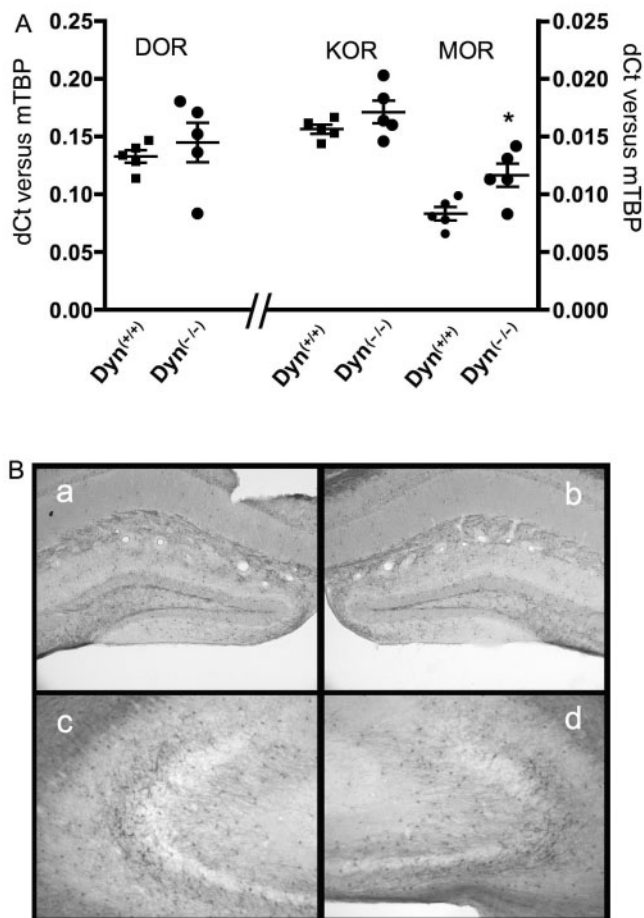
Fig. 1 Compensatory alterations in the opioid receptor system of the hippocampus in $Dyn^{-/-}$ mice. Panel **A** depicts the expression levels of DOR, KOR and MOR mRNA in the hippocampus of wild-type (squares) and knock-out (circles) mice. No differences were observed in the expression of DOR and KOR mRNAs. MOR receptor mRNA was expressed at very low levels in $Dyn^{+/+}$ mice, however increased by 40% in $Dyn^{-/-}$ mice. Data represent mean dCt of 3 replicates versus mouse TATA box binding protein (mTBP) mRNA. *$p \leqslant 0.05$ versus wild-type. Comparison of KOR immunoreactivities (**B**) in dorsal hippocampus of $Dyn^{+/+}$ (a,c) and $Dyn^{-/-}$ mice (b,d). No obvious changes were detected in KOR staining, indicating minor compensatory adaptations of this receptor in the $Dyn^{-/-}$ mice.

selective agonist SNC80 (2 mg/kg, i.p.) 1 h before PTZ infusion resulted in a markedly reduced seizure threshold of 17.5 ± 1.22 mg PTZ/kg ($n = 6$) (Fig. 1C). Noteworthy, none of these animals showed any signs of spontaneous seizure activity. To investigate potential compensatory changes on the level of DOR, we included a group of $Dyn^{+/+}$ mice treated with SNC80 prior to PTZ infusion, yielding a seizure threshold of 23.8 ± 1.01 mg PTZ/kg ($n = 5$; Fig. 1C). Treatment of $Dyn^{-/-}$ mice with the MOR selective agonist DAMGO 30 min before infusion resulted in an unchanged seizure threshold of 32.5 ± 1.68 mg PTZ/kg ($n = 6$; Fig. 1C). Efficiency of drug treatment was controlled through animal behaviour.

Fig. 2 Altered seizure behaviour in Dyn$^{-/-}$ mice. Panel **A** depicts the differences in seizure threshold as obtained by tail-vein infusion of PTZ. While heterozygous mice show only a tendency to reduced seizure threshold, Dyn$^{-/-}$ mice displayed a significantly lowered threshold. Panel **B** shows the rescue of this phenotype by ip injection of the KOR agonist U-50488 (Dyn$^{-/-}$ + U-50488). The action of the agonist is fully reversible by pre-treatment with the KOR specific antagonist GNTI (Dyn$^{-/-}$ + U-50488 + GNTI). The seizure threshold of Dyn$^{-/-}$ mice and wild-type mice treated with GNTI (Dyn$^{+/+}$ + GNTI) did not differ. The DOR specific agonist SNC80 markedly reduced seizure threshold in both Dyn$^{-/-}$ and Dyn$^{+/+}$ mice to a similar extend (panel **C**). The MOR specific agonist DAMGO did not influence the seizure threshold of Dyn$^{-/-}$ mice, although mice displayed a broad behavioural spectrum induced by MOR agonists. Our data clearly indicate that the main anticonvulsant activity of dynorphin is mediate by KOR. Panel **D** depicts the differences in acute seizure behaviour induced by ic injection of kainic acid. The left part shows the delay of seizure onset, while the right part illustrates the duration from the first to the last clonic seizure observed. *$p<0.05$; **$p<0.01$; ***$p<0.001$ versus untreated genotype matched control; ¥¥ $p<0.01$ versus Dyn$^{-/-}$; †† $p<0.01$ versus Dyn$^{-/-}$ + U-50488.

Mice receiving the KOR agonist were very calm, displaying typical drowsiness. GNTI entirely rescued this behavioural effect when given 20 h before U-50488. Animals treated with the KOR antagonist alone were highly alert and displayed some anxious like behaviour. Injection of SNC80 did not change behaviour dramatically; however, animals appeared more alert. DAMGO induced significant effects on mouse behaviour, including the MOR agonist typical 'Straub-tail', stiff hanging when picked up at the tail and hypoalgesia.

Intraperitoneal injection of a fixed dose of 30 mg PTZ/kg body weight resulted in a significantly different seizure response. Wild-type mice showed seizure severity scores of 2 (myoclonic jerks; $n=5$) and 3 (forelimb clonus; $n=2$) with only one animal displaying a clonic seizure (rating 4). In contrast, Dyn$^{-/-}$ mice reached a significantly ($P<0.01$; χ^2 test) higher seizure rating with three mice rated 3 and five animals displaying clonic seizures.

Seizure onset and duration

Seizure onset and duration was examined by intracisternal injection of 0.7 μg KA. In wild-type mice, clonic seizures were observed after 277 ± 45 s ($n=5$) and lasted for

13.9 ± 2.82 min ($n = 5$). Prodynorphin deficiency led to a faster onset (76 ± 36 s; $n = 5$; $P < 0.01$ versus wild-type) and a prolonged time of seizure activity (30.1 ± 3.56 min; $n = 5$; $P < 0.01$ versus wild-type; Fig. 1D). Animals injected with the same volume of saline recovered within a few seconds from anaesthesia and did not show any signs of seizure activity.

Seizure-related neurodegeneration and hippocampal reorganization

Potential neuroprotective effects of dynorphin were investigated in a model described as 'non-convulsant' status epilepticus induced by unilateral injection of 0.2 μg KA into the stratum radiatum of area CA1 of the dorsal hippocampus. In our hands, most of the treated mice showed myoclonic jerks and forelimb cloni when observed for gross behaviour 1 h and 1, 2 and 3 weeks after treatment. In both groups of animals, hippocampal neurodegeneration was prominent in CA1 and CA3c principal neurons of the ipsilateral dorsal hippocampus (Table 1, Figs 3 and 4). This goes in line with reduced numbers of SST-ir interneurons in these areas. Induction of neuropeptide Y (NPY) expression in mossy fibres of both hippocampi was observed in all KA-treated animals. Pathological changes were accompanied by sprouting of mossy fibres and a significant drop in immunoreactivity for ChB and NPY in the terminal field of mossy fibres as compared with the contralateral side (Fig. 4). Dyn$^{-/-}$ mice displayed a significantly broader extent of granule cell dispersion along the rostrocaudal axis of the ipsilateral hippocampus ($P = 0.0121$ versus WT; $n = 4$–6 per level; Table 1, Figs 3 and 4), but did not differ from Dyn$^{+/+}$ mice in maximal area covered by the GCL at the level of the injection site. The same holds true for the loss of Nissl stained and SST-ir neurons in the hilus ($P = 0.0077$ versus WT; $n = 4$–6 per level) and in area CA1 ($P = 0.0033$ versus WT; $n = 4$–6 per level). In addition, Dyn$^{-/-}$ mice showed markedly reduced SST-ir interneurons in the ipsilateral area CA3, while these neurons were still observed in wild-type mice ($P = 0.0021$ versus WT; $n = 4$–6 per level). Reduction of SST-ir interneurons in area CA1 ($P < 0.0001$ versus WT; $n = 4$–6 per level) as well as neurodegeneration of CA1 pyramidal cells ($P = 0.0053$ versus WT; $n = 4$–6 per level), accompanied by reduced NPY immunoreactivity in this subfield was observed in the contralateral hippocampus of Dyn$^{-/-}$ mice, but not in Dyn$^{+/+}$ mice (Table 1, Figs 3 and 4). Noteworthy, Dyn$^{-/-}$ mice displayed a significantly stronger reduction of Nissl stained neurons in the contralateral hilus ($P = 0.0133$ versus WT; $n = 4$–6 per level), while no reduction of SST-ir neurons was observed. No difference was observed in the reduction of SST-ir neurons in contralateral area CA3. In the ipsilateral dorsal hippocampus, marked changes in patterns of immunoreactivity for ChB and NPY were evident (Fig. 4).

Table I Neuropathology and morphology after local kainate injection

	Dyn$^{+/+}$ saline	Dyn$^{-/-}$ saline	Dyn$^{+/+}$ ipsilat	Dyn$^{-/-}$ ipsilat.	Dyn$^{+/+}$ contralat	Dyn$^{-/-}$ contralat
GCL area (μm²)	133 908 ± 13 591 (8)	115 843 ± 6669 (8)	319 359 ± 54 049 (6)**	378 886 ± 68 300 (6)***	153 389 ± 22 156 (6)	179 445 ± 22 456 (6)
Hilar neurons	37 ± 1.6 (7)	36 ± 1.6 (5)	1.7 ± 0.9 (7)***	0 ± 0.2 (6)***	19 ± 4.8 (7)***	22 ± 0.7 (6)**
CA1 cell number	51 ± 2.8 (7)	62 ± 2.9 (5)	1 ± 1.0 (6)***	1 ± 0.7 (6)***	48 ± 7.7 (7)	27 ± 6.8 (6)*** †
CA3a cell number	60 ± 3.5 (7)	58 ± 3.3 (5)	37 ± 5.5 (8)***	39 ± 2.2 (6)*	47 ± 1.8 (8)	53 ± 1.4 (6)
CA3b cell number	37 ± 2.5 (7)	43 ± 3.5 (5)	30 ± 4.7 (7)	32 ± 4.3 (6)	37 ± 4.3 (7)	41 ± 1.1 (6)
CA3 ccell number	43 ± 4.0 (7)	48 ± 3.5 (5)	8 ± 4.3 (8)***	3 ± 1.4 (6)***	38 ± 2.7 (8)	43 ± 4.5 (6)
SST-ir cells in Hilus	20 ± 1.1 (8)	18 ± 0.7 (9)	3 ± 1.6 (7)***	0 ± 0.9 (6)***	20 ± 1.3 (7)	18 ± 1.6 (6)
SST-ir cells in area CA3	31 ± 2.6 (8)	31 ± 3.5 (9)	21 ± 4.0 (8)	5 ± 2.2 (6)*** †	35 ± 4.2 (8)	28 ± 2.0 (6)
SST-ir cells in area CA1	29 ± 2.8 (8)	34 ± 2.6 (9)	7 ± 2.0 (7)***	4 ± 1.1 (6)***	31 ± 1.6 (7)	18 ± 1.3 (6)*** ††

The area of the granule cell layer (GCL) was taken as measure for dispersion, all other measurements assess specific cell groups. Data represent mean ± SEM (n) of data gained from section near the injection site (1.7–1.9 mm behind bregma) to measure maximal changes. *$P < 0.05$; **$P < 0.01$; ***$P < 0.001$ versus saline-treated genotype matched control; †$P < 0.05$; ††$P < 0.01$ versus wild-type (shaded fields).
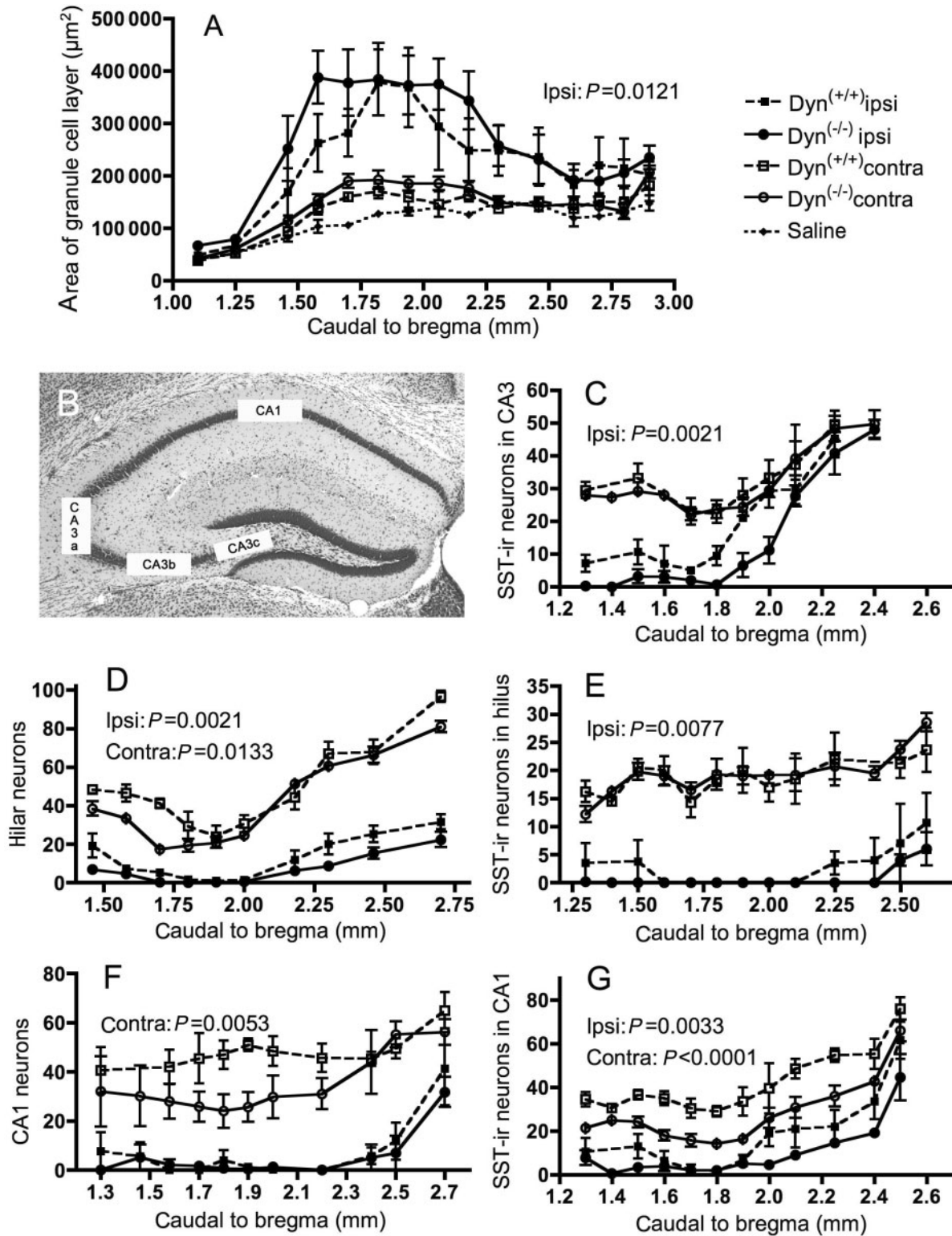
Fig. 3 Stereological analysis of neuronal loss and granule cell dispersion 3 weeks after unilateral intrahippocampal injection of KA. Panel **A** depicts alterations in the total area of the granule cell layer along the rostro-caudal axis of the dorsal hippocampus. Panels **B** outlines the areas (125μm length, full width) counted for the respective subfield of pyramidal cell layer. Panel **C** depicts numbers of SST-ir positive neurons in area CA3. Counts of scattered neurons in the hilus as detected by Nissl stain and SST immunocytochemistry are in panels **D** and **E**, respectively. Numbers of CA1 principle neurons are depicted in panels **F**, respectively. Panel **G** depicts numbers of SST-ir cells in area CA1. Note the increased extension of histological and pathological alterations along the rostro-caudal axis in Dyn$^{-/-}$ mice. In the ipsilateral hippocampus CA1 SST-ir neurons are lost in both phenotypes, while CA3 SST-ir cells are mostly spared in wild-type mice. Neurodegeneration in the contralateral hippocampus was seen only in Dyn$^{-/-}$ mice, affecting SST-ir and pyramidal cells in CA1 (Panel **D**). Distance to Bregma was evaluated by comparison to the atlas of Paxinos and Franklin. The legend given in (**A**) applies for all curves.

S. Loacker *et al.*
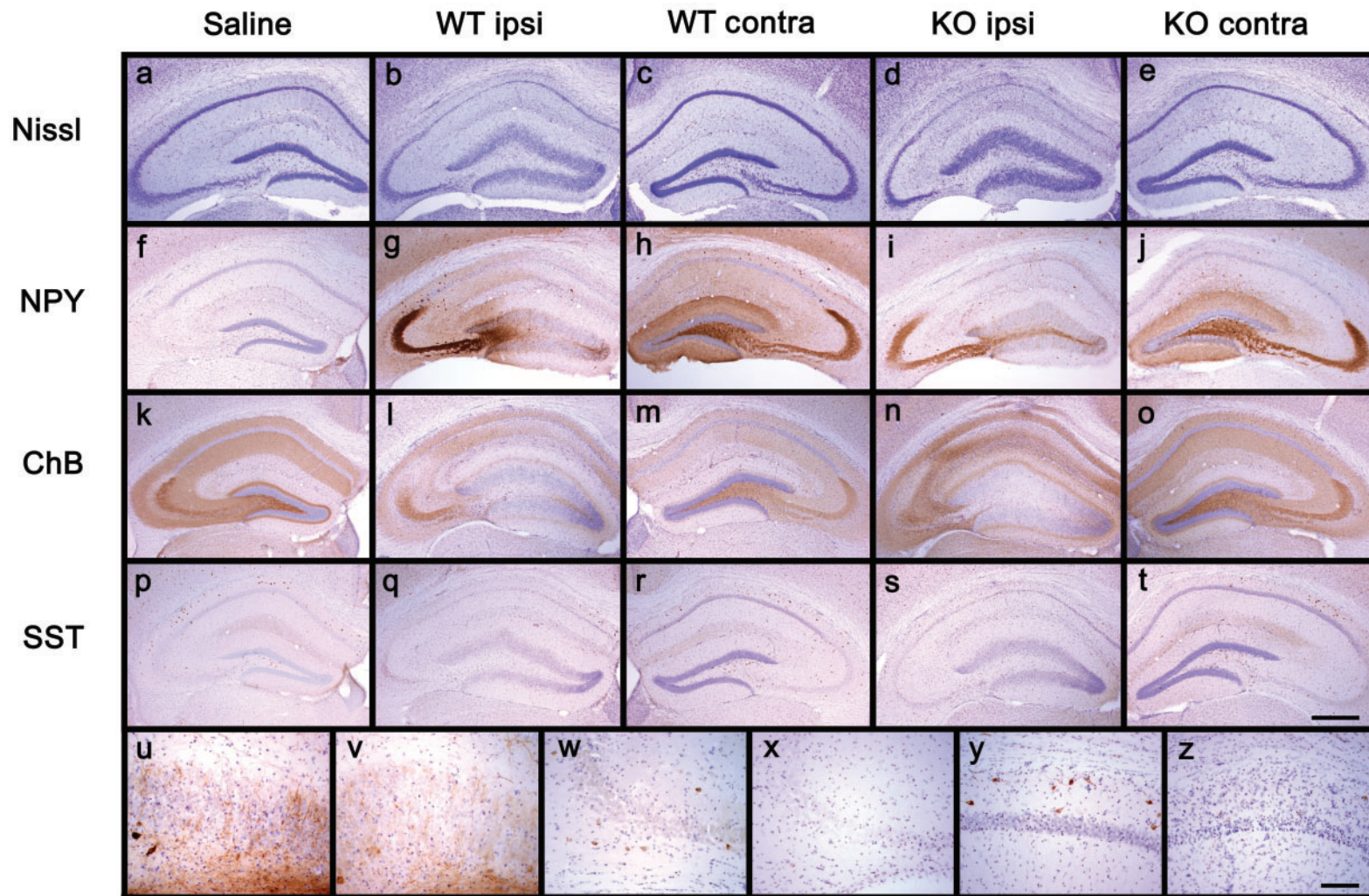
Fig. 4 Neuropathological and neurochemical alterations 3 weeks after intrahippocampal injection of KA. Photomicrographs obtained from $40\mu m$ sections of the dorsal hippocampus near the injection site (about 1.8 mm caudal to bregma) after Nissl staining (**A–E**) and immunohistochemical staining for NPY (**F–J;U,V**), ChB (**K–O**) and SST (**P–T;W–Z**) are depicted for saline injected controls (**A,F,K,P**), KA injected wild-type mice (ipsilateral: **B,G,L,Q,U,W**; contralateral: **C,H,M,R,Y**), and Dyn$^{-/-}$ mice (ipsilateral: **D,I,N,S,V,X**; contralateral: **E,J,O,T,Z**). Immunohistochemical sections were slightly counterstained with Cressyl violet for better identification of structures. Note the massive loss of CA1 and CA3c pyramidal neurons, accompanied by significant dispersion of the granule cell layer in the ipsilateral hippocampus of both strains (**B, D**). NPY immunoreactivity is restricted to interneurons in the saline treated control group, while it is highly expressed in granule cells of epileptic animals and overexpressed in surviving interneurons (**U,V**). The patches of reduced immunoreactivity in the ipsilateral hippocampi reflect loss of interneurons and granule cells. This loss of interneurons becomes also evident in the SST staining, while rearrangements in the principal cell layers are reflected in altered expressions patterns of ChB. Higher magnification micrographs in the lowest panel depict NPY immunoreactivity in the upper blades of the ipsilateral granule cells layer of wild-type (**U**) and Dyn$^{-/-}$ mice (**V**). Note the strong dispersion of granule cells, accompanied by mossy fiber sprouting (indicated by NPY immunoreactivity in the inner molecular layer) and loss of GABAergic interneurons. SST immunostaining of the ipsilateral area CA3a/b and contralateral area CA1 is shown for wild-type (**W,Y**) and Dyn$^{-/-}$ mice (**X,Z**), respectively. Note the increased loss of SST positive interneurons and the loss of CA1 pyramidal neurons in Dyn$^{-/-}$ mice. Bar in (**T**) for (**A–T**) $= 500\,\mu m$; in (**Z**) for (**U–Z**) $= 100\,\mu m$.

Table 2 Kindling progression in wild-type and $Dyn^{-/-}$ mice

Day	1	3	5	7	9	12	14	16	19	21	23	26	28	30	33	35
Injection no.	1	2	3	4	5	6	7	8	9	10	11	12	13	14	15	16
$Dyn^{+/+}$																
Rating 0	4	3	3	2	–	–	–	–	–	–	–	–	–	–	–	–
Rating 1	5	6	6	6	8	6	3	1	1	–	–	–	–	–	–	–
Rating 2	–	–	–	1	1	3	5	8	8	8	8	7	8	8	8	8
Rating 3	–	–	–	–	–	–	–	–	–	1	1	2	1	1	1	1
Rating 4	–	–	–	–	–	–	–	–	–	–	–	–	–	–	–	–
Rating 5	–	–	–	–	–	–	–	–	–	–	–	–	–	–	–	–
$Dyn^{-/-}$																
Rating 0	1	1	1	1	–	–	–	–	–	–	–	–	–	–	–	–
Rating 1	7	7	5	2	2	–	–	–	–	–	–	–	–	–	–	–
Rating 2	–	–	2	4	4	5	3	2	–	–	–	–	–	–	–	–
Rating 3	–	–	–	1	2	3	5	6	8	7	8	6	6	6	5	5
Rating 4	–	–	–	–	–	–	–	–	–	1	–	2	2	2	3	2
Rating 5	–	–	–	–	–	–	–	–	–	–	–	–	–	–	–	1
Significance					*	**	*	**	***	**	***	**	**	**	**	**

Nine wild-type and eight $Dyn^{-/-}$ mice were treated three times a week with 20 mg PTZ/kg bodyweight. Numbers indicate animals showing the respective seizure rate. For statistical analysis, the χ^2 test was applied. * $P < 0.05$; ** $P < 0.01$; *** $P < 0.001$ versus wild-type.

PTZ kindling

Classical PTZ kindling progression was investigated over a period of 5 weeks (Table 2). The kindling dose was established in pre-experiments. At a dose of 20 mg/kg wild-type mice rarely exceeded rating 2 seizures with five out of nine mice displaying rating 3 seizures once or twice within the time investigated (Table 2). On the other hand, prodynorphin-deficient mice showed clonic seizures beginning from injection 10, with six out of eight mice displaying at least one clonic seizure within 5 weeks. Furthermore, the frequency of mice exhibiting higher seizure scores in the knockout group was significantly increased from the fifth injection (Table 2). The kindling progression in $Dyn^{-/-}$ mice was similar to that observed in five wild-type mice injected with 25 mg PTZ/kg in dose-finding experiments (data not shown).

Discussion

Our data show decreased seizure threshold in the PTZ tail-vein infusion model and increased seizure activity in the acute KA model in prodynorphin-deficient mice. This is accompanied by increased neuropathological and morphological changes in a chronic epilepsy model. In line with this, kindling progression is significantly faster in $Dyn^{-/-}$ mice as in wild-type littermates in the classical PTZ kindling model. Thus we propose an anticonvulsant action of endogenous prodynorphin-derived peptides. Application of DOR-, KOR- and MOR-specific agonists and antagonists clearly identifies KOR as the mediators of these effects.

The correctness of the prodynorphin knockout became evident from the lack of prodynorphin mRNA and dynorphin A immunoreactivity. Potential compensatory changes in the expression of opioid receptor mRNAs in the hippocampus are restricted to MOR, which is increased by about 40% in our $Dyn^{-/-}$ mice. In contrast, no increase in MOR binding was observed in other $Dyn^{-/-}$ mice (Clarke et al., 2003). However, MOR receptor mRNA is expressed at low levels, and even at an elevated expression level, no influence of the MOR agonist on the seizure threshold in the PTZ tail-vein infusion model is detectable. The inference of no significant alteration in DOR functions in relation to seizure threshold is supported by the finding of a comparable reduction in $Dyn^{-/-}$ and $Dyn^{+/+}$ mice by the DOR normal type agonist SNC80. Unchanged KOR expression and distribution becomes evident from RT-PCR and immunocytochemistry. Normal functioning of these receptors is suggested by the full reversibility of the KOR agonist U-50488 action through the KOR antagonists GNTI.

Although there is increasing evidence for anti-ictal functions of prodynorphin-derived peptides (Seyfried and Glaser, 1985; Siggins et al., 1986; Tortella, 1988; Tortella and Long, 1988; Kai et al., 1998; Stogmann et al., 2002; Solbrig and Koob, 2004; Solbrig et al., 2006), several questions could not be answered by pharmacological approaches. These open questions are mostly related to activation of DOR and MOR, but also to direct interactions of endogenous dynorphin with NMDA receptors. Thus, application of DOR agonists causes seizures (Comer et al., 1993), on the other hand the anticonvulsant action of components within the cerebrospinal fluid of rats after seizures was inhibited by the addition of DOR antagonists (Tortella and Long, 1988). Dynorphin may inhibit the function of GABAergic interneurons through activation of MOR and KOR. The resulting inhibition of GABA release would facilitate seizures, on the other hand, desynchronization of interneurons might be beneficial in epilepsy

(Aradi *et al.*, 2002). Reports of dynorphin actions on NMDA receptors are also controversial. While Kanemitsu *et al.* (2003) suggested pH dependent inhibition of NMDA receptors, others propose stimulatory activities of dynorphin on NMDA responses (Caudle and Isaac, 1988; Shukla *et al.*, 1997; Woods *et al.*, 2006). Thus, the overall effect of endogenous prodynorphin-derived peptides was still controversial. We now showed anticonvulsant and neuroprotective functions of endogenous prodynorphin derived peptides in different models of epileptogenesis, acute seizures and chronic epilepsy. In addition, our data clearly indicate that anticonvulsant actions of the endogenous prodynorphin-derived peptides are predominantly mediated via KOR. Thus, decrease in seizure threshold observed in Dyn$^{-/-}$ mice could be completely rescued by the specific KOR agonist U-50488, but not by the MOR-specific agonist DAMGO. MOR are supposed to be expressed almost exclusively on specific subgroups of GABAergic interneurons in area CA1 (Drake and Milner, 1999, 2002). Noteworthy, the DAMGO dose and time interval to infusion used in our study was effective in reducing electrically induced seizures in C57Bl/6 mice (Yokoyama *et al.*, 1992). However, their findings stand in contradiction to results obtained in other groups. Thus, activation of MOR inhibited IPSPs and facilitated the propagation of excitatory activity in principal cells of slice preparations obtained from rat hippocampus. On the other hand, this facilitation was prevented by GABA$_A$ receptor antagonists like bicuculline (McQuiston and Saggau, 2003). Thus, the functions of MOR activation remain contradictive and have no influence in our model applying the GABA$_A$ receptor antagonist PTZ.

The DOR-specific agonist SNC80 by itself decreased the seizure threshold. Early works suggest disinhibition of principal neurons in CA1 and CA3 due to inhibition of inhibitory interneurons as main cause for the proconvulsant effects of endorphins and enkephalins acting via DOR (Siggins *et al.*, 1986). This may depend on the modulation of potassium and hyperpolarization-activated cation currents (Svoboda and Lupica, 1998). A more recent study showed that the proconvulsant effect of DOR agonists depends on the activation of constitutive NO synthase (Khavandgar *et al.*, 2002). DOR activation may also directly influence glutamatergic neurotransmission. Thus, DOR activation modulates the functions of voltage-dependent sodium channels (Remy *et al.*, 2004) as well as of the glutamate transporter EAAC1 (Xia *et al.*, 2006). One or several of these effects may be responsible for the reduced seizure threshold observed in SNC80-treated animals. Blocking of DOR with the specific antagonist naltrindole did not result in altered seizure behaviour in mouse and rat (Comer *et al.*, 1993; Mazarati *et al.*, 1999; Manocha *et al.*, 2003). Minor endogenous activation of DOR in the hippocampus is also supported by the low expression of proenkephalin in naive mice. In any case, the reduction in seizure threshold through pharmacological activation of DOR appears independent of the presence or absence of prodynorphin-derived peptides.

The effect of U-50488 was completely reversed by the KOR-specific antagonist GNTI, clearly indicating the predominance of KOR in the anti-ictal functions of endogenous prodynorphin-derived peptides. Our data rule out a significant contribution of MOR-mediated effects to the seizure regulation through dynorphin, although this receptor is expressed about 40% higher in Dyn$^{-/-}$ mice. Minor action of prodynorphin-derived peptides on DOR is suggested by the fact, that the seizure threshold of Dyn$^{-/-}$ mice treated with the KOR selective agonist U-50488 did not significantly differ from wild-type mice, although proconvulsant effects of dynorphin acting on DOR should be erased through prodynorphin knockout.

Although there is some evidence for anticonvulsant activity of dynorphin (for review *see* Solbrig and Koob, 2004), one of the major open questions is the receptor mediating these effects. KOR density is rather low in the hippocampus, on the other hand their distribution is strategically perfect in terms of dampening excitation in the limbic circuitry. Indeed, KOR are also capable to block LTP in the hippocampus (Wagner *et al.*, 1993). Presynaptic KOR are located on terminals of perforant path fibres, mossy fibres and pyramidal neurons (Drake *et al.*, 1994; Terman *et al.*, 2000). CA1 and CA3 neurons also contain KOR mRNA (Mansour *et al.*, 1994). Presynaptic KOR of perforant path fibres and mossy fibres, as well as postsynaptic KOR on CA3 pyramidal neurons are potential targets for dynorphin released from mossy fibres during seizures. Presynaptic activation of KOR decreases N-, L- and P/Q-type Ca^{++} currents (Rusin *et al.*, 1997), resulting in reduction of glutamate release. Stimulation of voltage-gated K$^+$ channels through postsynaptic KOR was proposed for pyramidal neurons (Moore *et al.*, 1994; Madamba *et al.*, 1999). In sum these effects, together with other potentially anticonvulsant sites of KOR action like the thalamus or substantia nigra cause an ~15% higher seizure threshold in wild-type mice as compared with Dyn$^{-/-}$ animals. Unfortunately, no data addressing seizure behaviour in KOR knockout mice are available by now.

The differences between the genotypes observed in the model of intrahippocampal KA injection are in agreement with the potential sites of action for dynorphin. Thus, the GCL displayed augmented dispersion and reduction of SST-ir interneurons was increased in the target area of mossy fibres, CA3. In general, SST-ir neurons were significantly more reduced in Dyn$^{-/-}$ mice, which might be related to higher release of glutamate, but also directly to the lack in dynorphin, as these SST/NPY neurons were reported to express KOR in rat (Racz and Halasy, 2002). In any case, it should be kept in mind that reduced numbers of SST-ir cells does not necessarily reflect neuronal death, but may also reflect a decrease in SST levels below detection limit. Interestingly, no change in numbers of SST-ir cells was observed in the contralateral hilus,

although there was a marked drop in Nissl-stained neurons. In addition, Dyn$^{-/-}$ mice also show significant loss of neurons in the contralateral hippocampal area CA1, potentially reflecting increased commissural excitatory signalling due to loss of dynorphin. Marked stimulation of the contralateral hippocampus in both groups of animals was indicated by the appearance of NPY immunoreactivity in mossy fibres of both hippocampi in all KA-treated animals. Taken together, the differences in neuropathology suggest a higher excitatory level of the limbic circuit in Dyn$^{-/-}$ mice. This is in line with other reports of the effects of opioids on hippocampal excitability (Wagner et al., 1993; Terman et al., 2000).

Partial loss of control on excitatory neurotransmission through perforant path and mossy fibre synapses may well account also for the faster kindling observed in the Dyn$^{-/-}$ mice. Actually the kindling rate in Dyn$^{-/-}$ mice at 20 mg PTZ/kg is significantly faster than in wild-type littermates treated with 20 mg PTZ/kg, but comparable with that observed in wild-type mice treated with 25 mg PTZ/kg in dose-finding experiments (data not shown).

Also under debate is the finding of increased seizure susceptibility in humans with a prodynorphin gene promoter polymorphism resulting in reduced expression of prodynorphin (Stogmann et al., 2002). Similar results were reported by Gambardella et al. (2003). Although the specific associations reported by Stogmann et al. (2002) could not be reproduced in more recent studies (Cavalleri et al., 2005), the authors state that the mutation in the prodynorphin promoter may act as a general risk factor for epilepsy. Noteworthy, only 50 patients out of 752 investigated in this study matched the phenotype investigated by Stogmann et al. (2002). Our data support the findings of Stogmann et al. (2002). On the other hand, the about 25% reduction in prodynorphin mRNA observed in heterozygous Dyn$^{+/-}$ mice (data not shown) yield only a tendency to reduced seizure threshold. This might explain the difficulties to reproduce the observations of Stogmann and colleagues.

Conclusions

Our data clearly indicate that endogenous prodynorphin-derived peptides acting on kappa opioid receptors contribute significantly to the control of excitatory neurotransmission in hippocampal granule cells in naive animals and during epileptogenesis. Thus, kappa opioid receptors might represent a target for the treatment of mTLE, potentially also suitable to reduce the progression of the disease. However, drugs will have to be highly selective for KOR with no activity on DOR in therapeutic doses to avoid proconvulsant effects through DOR activation. DOR antagonism of such drugs might look beneficial at first sight, but may cause severe side-effects related to pain or depression.

Supplementary material

Supplementary material is available at Brain Online.

Acknowledgements

References

Aradi I, Santhakumar V, Chen K, Soltesz I. Postsynaptic effects of GABAergic synaptic diversity: regulation of neuronal excitability by changes in IPSC variance. Neuropharmacology 2002; 43: 511–22.

Bouilleret V, Ridoux V, Depaulis A, Marescaux C, Nehlig A, Le Gal La Salle G. Recurrent seizures and hippocampal sclerosis following intrahippocampal kainate injection in adult mice: electroencephalography, histopathology and synaptic reorganization similar to mesial temporal lobe epilepsy. Neuroscience 1999; 89: 717–29.

Caudle RM, Isaac L. A novel interaction between dynorphin(1–13) and an N-methyl-D-aspartate site. Brain Res 1988; 443: 329–32.

Cavalleri GL, Lynch JM, Depondt C, Burley MW, Wood NW, Sisodiya SM, et al. Failure to replicate previously reported genetic associations with sporadic temporal lobe epilepsy: where to from here? Brain 2005; 128: 1832–40.

Chavkin C, James IF, Goldstein A. Dynorphin is a specific endogenous ligand of the kappa opioid receptor. Science 1982; 215: 413–5.

Clarke S, Zimmer A, Zimmer AM, Hill RG, Kitchen I. Region selective up-regulation of micro-, delta- and kappa-opioid receptors but not opioid receptor-like 1 receptors in the brains of enkephalin and dynorphin knockout mice. Neuroscience 2003; 122: 479–89.

Comer SD, Hoenicke EM, Sable AI, McNutt RW, Chang KJ, De Costa BR, et al. Convulsive effects of systemic administration of the delta opioid agonist BW373U86 in mice. J Pharmacol Exp Ther 1993; 267: 888–95.

DePaoli AM, Hurley KM, Yasada K, Reisine T, Bell G. Distribution of kappa opioid receptor mRNA in adult mouse brain: an in situ hybridization histochemistry study. Mol Cell Neurosci 1994; 5: 327–35.

Drake CT, Milner TA. Mu opioid receptors are in somatodendritic and axonal compartments of GABAergic neurons in rat hippocampal formation. Brain Res 1999; 849: 203–15.

Drake CT, Milner TA. Mu opioid receptors are in discrete hippocampal interneuron subpopulations. Hippocampus 2002; 12: 119–36.

Drake CT, Terman GW, Simmons ML, Milner TA, Kunkel DD, Schwartzkroin PA, et al. Dynorphin opioids present in dentate granule cells may function as retrograde inhibitory neurotransmitters. J Neurosci 1994; 14: 3736–50.

Gackenheimer SL, Suter TM, Pintar JE, Quimby SJ, Wheeler WJ, Mitch CH, et al. Localization of opioid receptor antagonist [3H]-LY255582 binding sites in mouse brain: comparison with the distribution of mu, delta and kappa binding sites. Neuropeptides 2005; 39: 559–67.

Gambardella A, Manna I, Labate A, Chifari R, Serra P, La Russa A, et al. Prodynorphin gene promoter polymorphism and temporal lobe epilepsy. Epilepsia 2003; 44: 1255–6.

Henriksen SJ, Chouvet G, McGinty J, Bloom FE. Opioid peptides in the hippocampus: anatomical and physiological considerations. Ann N Y Acad Sci 1982; 398: 207–20.

Jewett DC, Grace MK, Jones RM, Billington CJ, Portoghese PS, Levine AS. The kappa-opioid antagonist GNTI reduces U50,488-, DAMGO-, and deprivation-induced feeding, but not butorphanol- and neuropeptide Y-induced feeding in rats. Brain Res 2001; 909: 75–80.

Jones RM, Portoghese PS. 5′-Guanidinonaltrindole, a highly selective and potent kappa-opioid receptor antagonist. Eur J Pharmacol 2000; 396: 49–52.

Kai T, Onishi H, Koide S, Katayama M, Yamagami S. Developmental and regional alteration of kappa-opioid receptors in seizure-susceptible EL mouse brain. Neurochem Res 1998; 23: 163–8.

Kanemitsu Y, Hosoi M, Zhu PJ, Weight FF, Peoples RW, McLaughlin JS, et al. Dynorphin A inhibits NMDA receptors through a pH-dependent mechanism. Mol Cell Neurosci 2003; 24: 525–37.

Khavandgar S, Homayoun H, Dehpour AR. The role of nitric oxide in the proconvulsant effect of delta-opioid agonist SNC80 in mice. Neurosci Lett 2002; 329: 237–9.

Kwan P, Brodie MJ. Early identification of refractory epilepsy. N Engl J Med 2000; 342: 314–9.

Kwan P, Sander JW. The natural history of epilepsy: an epidemiological view. J Neurol Neurosurg Psychiatry 2004; 75: 1376–81.

Lin S, Boey D, Lee N, Schwarzer C, Sainsbury A, Herzog H. Distribution of prodynorphin mRNA and its interaction with the NPY system in the mouse brain. Neuropeptides 2006; 40: 115–23.

Madamba SG, Schweitzer P, Siggins GR. Dynorphin selectively augments the M-current in hippocampal CA1 neurons by an opiate receptor mechanism. J Neurophysiol 1999; 82: 1768–75.

Maggi R, Limonta P, Dondi D, Martini L, Piva F. Distribution of kappa opioid receptors in the brain of young and old male rats. Life Sci 1989; 45: 2085–92.

Manocha A, Mediratta PK, Sharma KK. Studies on the anticonvulsant effect of U50488H on maximal electroshock seizure in mice. Pharmacol Biochem Behav 2003; 76: 111–7.

Mansour A, Fox CA, Meng F, Akil H, Watson SJ. Kappa 1 receptor mRNA distribution in the rat CNS: comparison to kappa receptor binding and prodynorphin mRNA. Mol Cell Neurosci 1994; 5: 124–44.

Mazarati A, Liu H, Wasterlain C. Opioid peptide pharmacology and immunocytochemistry in an animal model of self-sustaining status epilepticus. Neuroscience 1999; 89: 167–73.

McNamara JO. Emerging insights into the genesis of epilepsy. Nature 1999; 399: A15–22.

McQuiston AR, Saggau P. Mu-opioid receptors facilitate the propagation of excitatory activity in rat hippocampal area CA1 by disinhibition of all anatomical layers. J Neurophysiol 2003; 90: 1936–48.

Moore SD, Madamba SG, Schweitzer P, Siggins GR. Voltage-dependent effects of opioid peptides on hippocampal CA3 pyramidal neurons in vitro. J Neurosci 1994; 14: 809–20.

Nilsen KE, Cock HR. Focal treatment for refractory epilepsy: hope for the future? Brain Res Brain Res Rev 2004; 44: 141–53.

Paxinos G, Franklin KBJ. The mouse brain in stereotaxic coordinates. San Diego: Academic Press; 2001.

Polkey CE. Clinical outcome of epilepsy surgery. Curr Opin Neurol 2004; 17: 173–8.

Racz B, Halasy K. Kappa opioid receptor is expressed by somatostatin- and neuropeptide Y-containing interneurons in the rat hippocampus. Brain Res 2002; 931: 50–5.

Remy C, Remy S, Beck H, Swandulla D, Hans M. Modulation of voltage-dependent sodium channels by the delta-agonist SNC80 in acutely isolated rat hippocampal neurons. Neuropharmacology 2004; 47: 1102–12.

Rusin KI, Giovannucci DR, Stuenkel EL, Moises HC. Kappa-opioid receptor activation modulates Ca2 + currents and secretion in isolated neuroendocrine nerve terminals. J Neurosci 1997; 17: 6565–74.

Schwarzer C, Berresheim U, Pirker S, Wieselthaler A, Fuchs K, Sieghart W, et al. Distribution of the major gamma-aminobutyric acid(A) receptor subunits in the basal ganglia and associated limbic brain areas of the adult rat. J Comp Neurol 2001; 433: 526–49.

Schwarzer C, Sperk G, Rauca C, Pohle W. Neuropeptide Y and somatostatin immunoreactivity in the rat hippocampus after moderate hypoxia. Naunyn Schmiedebergs Arch Pharmacol 1996; 354: 67–71.

Seyfried TN, Glaser GH. A review of mouse mutants as genetic models of epilepsy. Epilepsia 1985; 26: 143–50.

Shukla VK, Prasad JA, Lemaire S. Nonopioid motor effects of dynorphin A and related peptides: structure dependence and role of the N-methyl-D-aspartate receptor. J Pharmacol Exp Ther 1997; 283: 604–10.

Siggins GR, Henriksen SJ, Chavkin C, Gruol D. Opioid peptides and epileptogenesis in the limbic system: cellular mechanisms. Adv Neurol 1986; 44: 501–12.

Solbrig MV, Adrian R, Baratta J, Lauterborn JC, Koob GF. Kappa opioid control of seizures produced by a virus in an animal model. Brain 2006; 129: 642–54.

Solbrig MV, Koob GF. Epilepsy, CNS viral injury and dynorphin. Trends Pharmacol Sci 2004; 25: 98–104.

Stogmann E, Zimprich A, Baumgartner C, Aull-Watschinger S, Hollt V, Zimprich F. A functional polymorphism in the prodynorphin gene promotor is associated with temporal lobe epilepsy. Ann Neurol 2002; 51: 260–3.

Svoboda KR, Lupica CR. Opioid inhibition of hippocampal interneurons via modulation of potassium and hyperpolarization-activated cation (Ih) currents. J Neurosci 1998; 18: 7084–98.

Terman GW, Drake CT, Simmons ML, Milner TA, Chavkin C. Opioid modulation of recurrent excitation in the hippocampal dentate gyrus. J Neurosci 2000; 20: 4379–88.

Tortella FC. Endogenous opioid peptides and epilepsy: quieting the seizing brain? Trends Pharmacol Sci 1988; 9: 366–72.

Tortella FC, Long JB. Characterization of opioid peptide-like anticonvulsant activity in rat cerebrospinal fluid. Brain Res 1988; 456: 139–46.

Wagner JJ, Terman GW, Chavkin C. Endogenous dynorphins inhibit excitatory neurotransmission and block LTP induction in the hippocampus. Nature 1993; 363: 451–4.

Weisskopf MG, Zalutsky RA, Nicoll RA. The opioid peptide dynorphin mediates heterosynaptic depression of hippocampal mossy fibre synapses and modulates long-term potentiation. Nature 1993; 365: 188.

WHO. Atlas: epilepsy care in the world. Geneva: Programme for Neurological Diseases and Neuroscience, Department of Mental Health and Substance Abuse, WHO; 2005.

Wollemann M, Benyhe S. Non-opioid actions of opioid peptides. Life Sci 2004; 75: 257–70.

Woods AS, Kaminski R, Oz M, Wang Y, Hauser K, Goody R, et al. Decoy peptides that bind dynorphin noncovalently prevent NMDA receptor-mediated neurotoxicity. J Proteome Res 2006; 5: 1017–23.

Xia P, Pei G, Schwarz W. Regulation of the glutamate transporter EAAC1 by expression and activation of delta-opioid receptor. Eur J Neurosci 2006; 24: 87–93.

Yokoyama H, Onodera K, Suzuki T, Iinuma K, Watanabe T. Opioid mu-deficient CXBK mouse and the role of mu 1-receptors in electrically induced convulsions. Brain Res 1992; 595: 137–40.